Intensity fluctuations of midfrequency sound signals passing through moving nonlinear internal waves

Boris Katsnelson and Valery Grigorev
Voronezh State University, 1 Universitetskaya Square, Voronezh 394006, Russia
katz@phys.vsu.ru, grig@box.vsi.ru

James F. Lynch
Woods Hole Oceanographic Institution, Woods Hole, Massachusetts 02543
jlynch@whoi.edu

Abstract: The fluctuations of intensity of broadband pulses in the midfrequency range (2–4.5 kHz) propagating in shallow water in the presence of intense internal waves moving approximately along the acoustic track are considered. These pulses were received by two separate single hydrophones placed at different distances from the source (~4 and ~12 km) and in different directions. It is shown that the frequency spectra of the fluctuations for these hydrophones have different predominating frequencies corresponding with the directions of the acoustic track. Comparisons of experimental results with theoretical estimates demonstrate good consistency.

PACS numbers: 43.30.Re, 43.30.Es, 43.30.Cq [DKW]
Date Received: March 26, 2008 **Date Accepted:** July 16, 2008

1. Introduction

Fluctuations of the intensity of low frequency sound waves in the presence of intense internal waves moving along an acoustic track were considered in previous papers[1] (experimental observations) and[2] (theoretical analysis). It was shown that the hypothesis of mode coupling as the physical reason for the fluctuations explains the peculiarities of the spectrum of these fluctuations (i.e., existence and value of a predominating frequency, the arrival times, etc.).

For mid and high frequency sound waves, ray language should be used for the description of sound propagation in the presence of internal solitons (IS) moving along the acoustic track[2] as illustrated in Fig. 1. A source and receiver (*S* and *R*) of sound signals are placed in shallow water with some distance between them, with trajectories of typical rays coming from the source to receiver as shown in Fig. 1. In the presence of internal solitons moving along the acoustic track, we have some moving perturbation of the thermocline layer and correspondingly some perturbation of the trajectory of the rays. This perturbation depends on the position of the IS and on the types of rays. For example, if the soliton is at position A, then it causes a distortion of ray 3, whereas for position B of the soliton, ray 3 does not interact with it. So during the motion of the soliton there are temporal fluctuations of the sound intensity at the receiver. It is clear that the perturbation depends on the type of rays; for example, ray 3 interacts with the soliton more strongly than rays 1 and 2. It has been shown that the most significant perturbation is provided by the rays which are tangent to the thermocline layer (these rays will be called as "critical rays," corresponding to ray 3 in Fig. 1), whereas other rays (denoted as 1 and 2 in Fig. 1) give a comparatively small contribution to the fluctuations. So if the phase velocity v_t of the IS crest along the direction of the acoustic track (which is greater than the real velocity v of the IS, which is perpendicular to the wave front of the IS) is taken to be constant, then the most significant fluctuations of the sound amplitude at the receiver will take place with a period T_c determined by v_t and the cycle distance of the critical ray D_c: $T_c = D_c / v_t$. For real ocean conditions, $T_c \geqslant 10$ min, and so during the time of observation, there can be 5–10 oscillations of the

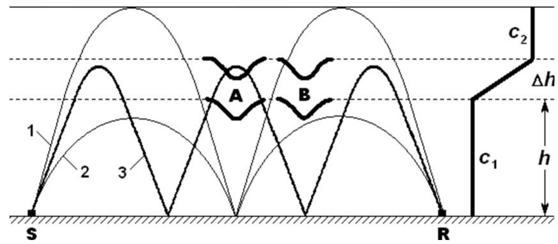

Fig. 1. Schematic of the interaction of an internal soliton with sound rays of different types radiated from a source placed at the bottom. Sound speed profile on the right side corresponds to a simplified one for SW06. We did not emphasize the small negative gradients in the upper and lower layers (seen in the experiment) in the profile graph, but they are evident in the ray trace results. Waveguide parameters are: $h \sim 60$ m, $\Delta h \sim 10$ m, $c_1 \sim 1480$ m/s, and $c_2 \sim 1525$ m/s.

sound intensity. A spectrum of this signal taken during the time of observation ($\sim$60 min) should contain set of maxima spanned by the value $\Omega_c \sim v_t/D_c$. The value of Ω_c is the "frequency of collisions" of the IS with the critical ray and can also be called the "predominating frequency." For typical conditions, $\Omega_c \leqslant 10$ cph.

An important feature of this spectrum is the dependence of the predominating frequency Ω_c on the angle between the direction of the acoustic track and the direction of propagation of the IS. Using this, it is possible to check this theory with an experiment where there are two acoustic tracks with different directions (two receivers for one and the same source) if they are crossed by the same soliton (or train of solitons). In this case we should have fluctuations of the same sequence of signals with different predominating frequencies, corresponding to the projections of the real velocity on the direction of the acoustic track. Such a situation took place in the SW06 experiment, along an acoustic track created by a source on the R/V KNORR.

2. The shallow water 2006 (SW06) experiment. Environmental data and soliton's parameters

The layout of the part of SW06 on 13 August during the time period 15:31–16:20 Greenwich mean time (GMT) is shown in Fig. 2. Positions of the source (R/V KNORR), two single hydrophone receiving units (SHRU1 and SHRU2) and thermistor strings (SW23, SW24, SW30,

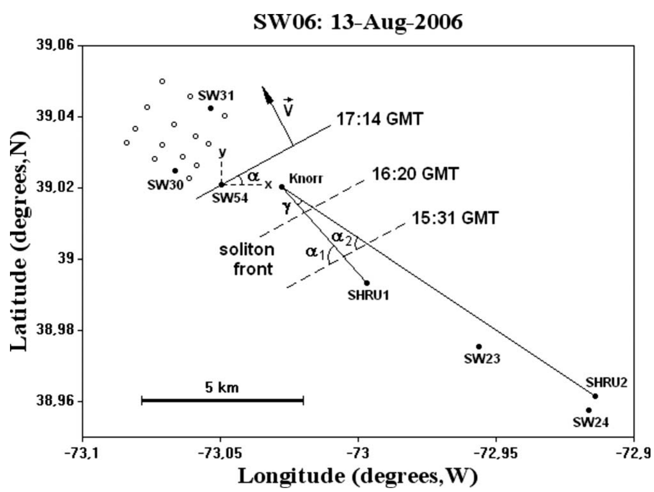

Fig. 2. Scheme of experiments with midfrequency pulses in SW06. Black straight lines denote acoustic tracks 1 (Knorr-SHRU1) and 2 (Knorr-SHRU2).

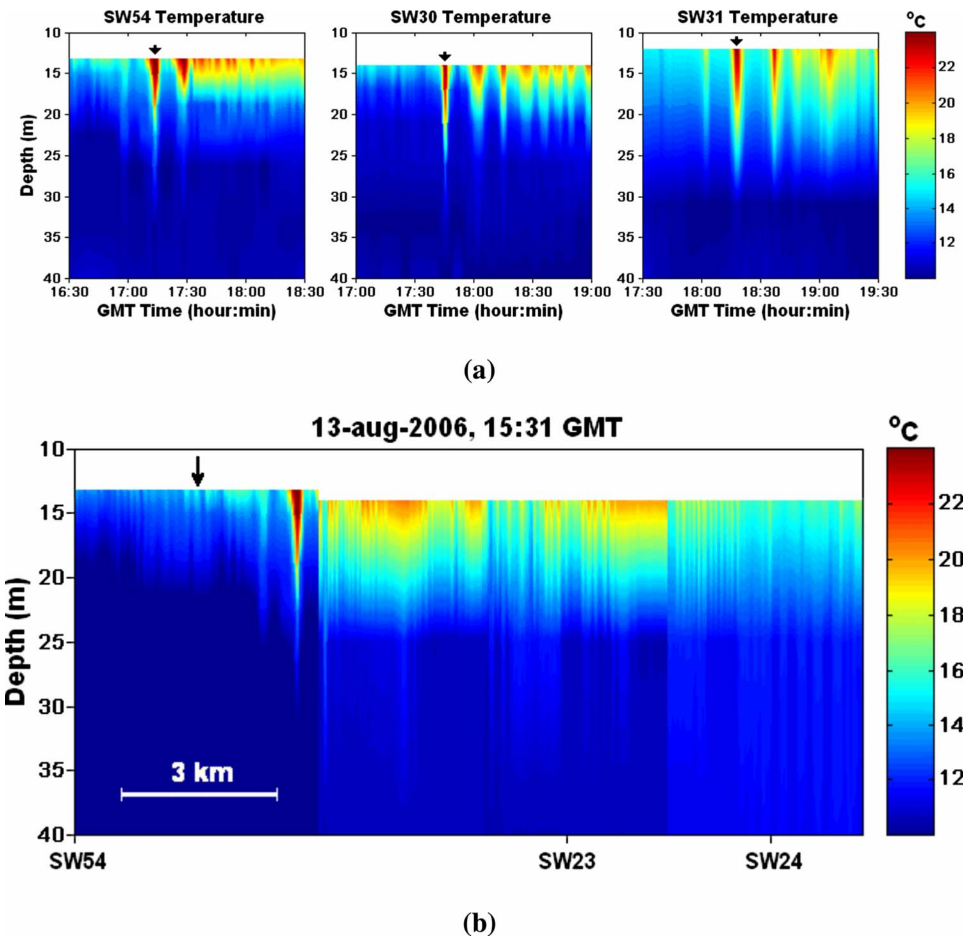

Fig. 3. (Color online) (a) Temperature records of an internal soliton at three thermistor strings. Color scale of temperature is shown at the right. (b) Reconstructed depth distribution of temperature for 15:31 GMT along a straight line between thermistor's sensors SW24-SW23-SW54. Black arrow denotes position of the soliton at 16:20 GMT.

SW31, SW54) are also shown in Fig. 2. The angle between the acoustic tracks is denoted by γ, and was found to be $\gamma \sim 15°$.

The behavior of internal waves was monitored by several thermistor strings, moored at different places. The temporal records of temperature depth distribution from the sensors denoted SW23, SW24, SW54, SW30, and SW31 (see Fig. 2) are used to find the shape of internal waves. During this time period, some solitons were registered. In Fig. 3(a) three temperature records of the soliton train are shown, which is moving approximately toward the coast. The moored sensors were reached by the first peak at different times [marked by arrows in Fig. 3(a)]. The different shapes of the temperature distribution demonstrate the evolution of the soliton train in time and space. It is easy to estimate the velocity and direction of propagation of the IS in a Cartesian coordinate system on the horizontal plane with the origin at mooring SW54. Suppose that the train or separate IS has a plane wave front directed at angle α with the X-axis, and moves with constant velocity v (Fig. 2). The given soliton consequently reaches sensor SW54, then SW30 and then SW31 [Fig. 3(a)]. The corresponding time differences between the points SW30 and SW31 from one side and SW54 from other side are ΔT_{30}=31 min and ΔT_{31} =63 min. In this case

$$\alpha = \arctan \frac{y_{30}\Delta T_{31} - y_{31}\Delta T_{30}}{x_{30}\Delta T_{31} - x_{31}\Delta T_{30}},$$

$$v = \frac{y_{30} - x_{30}\tan\alpha}{\Delta T_{30}} \cos\alpha,$$

where $x_{30}=-1477$ m, $y_{30}=456$ m, $x_{31}=-337$ m, and $y_{31}=2402$ m.

Taking into account experimental errors, we have approximately $\alpha \sim 29°$, $v \sim 0.6$ m/s.

For a more detailed analysis of internal waves outside of the acoustic track, the 14 thermistors SW04–SW17 can be used (shown in Fig. 2 by circles). In this case, the angle α changes during the motion from right to left in a sector from 26° to 44°, as a result of the variation of direction during the propagation and bending of the wave front. At the same time, along an acoustic track a comparatively constant direction of the wave front takes place, and for the following work we take $\alpha \sim 29°$.

Next, the spatial crossection of the internal waves along the straight line SW24-SW23-SW54 can be constructed for some fixed time, for example 15:31 GMT. Let us denote the temperature record at some point as $T^0(T,z)$, where T^0 is temperature and T is GMT. Within the framework of our approximation $T^0=T^0[T-T_0-(l-l_0)/v_l,z]$, where l is a length along the above mentioned direction, v_l is the corresponding projection of the real velocity v, and T_0, l_0 are some fixed GMT time and spatial position of the internal waves. Note that in spite of Fig. 3(a) showing some evolution of the IS propagating toward the coast, during our time of processing ($\sim$1 h) we can neglect this modification and consider the shape of the IS to be constant.

The reconstructed temperature distribution is shown in Fig. 3(b). According to our environmental picture, there is only one separate soliton at both acoustic tracks: KNORR-SHRU1 and KNORR-SHRU2 for the time interval, (15:31–16:20 GMT). Positions of the wave front of the soliton for 15:31 GMT and 16:20 GMT are shown in Fig. 2 by dotted lines and are also denoted in Fig. 3(b) (soliton itself and black arrow). The velocity of the soliton along this direction is about 0.7 m/s.

3. SW06 experiment. Midfrequency acoustical data and analysis

During our study period, a sequence of pulses was radiated consisting of 200 separate pulses in the frequency band 2–10 kHz. As was said above, these pulses were received independently at SHRU1 and SHRU2. The spectrum of radiated signals was in the band 2–10 kHz. However, for the processing, we use a sampling time $\delta t=0.000\,102\,4$ s, which corresponds to maximal frequency in the spectrum of $(2\delta t)^{-1}=4.88$ kHz. So only the intensity of received pulses in the band 2–4 kHz is considered here. The analysis above shows that the character of the fluctuations should not depend on the frequency in this band.

Let the received pulse have the sound pressure signature $p(t)$ with the spectrum

$$S(\omega) = \int_0^\tau p(t)\exp(i\omega t)dt. \tag{1}$$

Here, we take $\tau=0.1$ s (the approximate duration of the pulse) for both receivers. Formally speaking, an infinite time period should be taken; however, it is more sensible to take this reduced period because outside of this interval there is noise only. So the energy of the pulse (up to constant factor) is

$$E = \int_{\omega_1}^{\omega_2} |S(\omega)|^2 d\omega, \tag{2}$$

where $\omega_1=2$ kHz and $\omega_2=4$ kHz.

The energy of the received pulses fluctuates from pulse to pulse, as a function of GMT, so it is denoted as $E=E(T)$. The temporal dependence of the relative fluctuations is

$$\bar{E}(T) = \frac{E(T) - \langle E\rangle}{\langle E\rangle}, \tag{3}$$

where $\langle E\rangle = 1/\Delta T\int_0^{\Delta T} E(T)dT$ is the average energy for the time period $\Delta T=49$ min. The temporal dependence of the fluctuations of energy for both hydrophones is shown in Fig. 4

We see from Figs. 4(a) and 4(b) that the oscillations of the temporal dependence of the sound energy have a rather regular character. According to theory,[2] the frequency spectrum of the temporal behavior has predominating frequencies, corresponding to the quasiperiodical interaction of the sound pulse with the periodical ray structure of the sound field. The most significant interaction takes place for the critical ray, so the predominating frequency is determined by the time of motion of the pulse between adjacent maxima of the critical ray.

Let us consider the spectrum of fluctuations, or more exactly the amplitude of this spectrum

$$\bar{G}(\Omega) = \left| \int_0^{\Delta T} \bar{E}(T)\exp(i\Omega T)dT \right|. \tag{4}$$

The spectra for the temporal series from SHRU1 and SHRU 2 are shown in Fig. 4(c) in decibel (dB) units; more exactly, the values 10 log $\bar{G}(\Omega)$ are shown.

It is seen that both spectra are functions having a quasiperiodical structure in the frequency domain in the region below 30 cph. The positions of the maxima in the spectra corresponding to SHRU1 and SHRU2 are shifted. According to interpretation,[2] this is due to the different directions of the sound propagation relative to the direction of propagation of the internal solitons.

The predominating frequencies and the average shifts of the spectra can be estimated from the experimental data [Fig. 4(c)]. In particular maxima (harmonics) number 4 are shifted by 1.7 cph. For this case, $\Omega_c^1 \approx 3.58$ cph and $\Omega_c^2 \approx 4$ cph.

Let us consider the temporal dependence from the point of view of our theory, i.e., that the motion of the soliton is the reason for the fluctuations with a predominating frequency, and compare the estimation from Ref. 2 with the results of our observations.

A diagram of the experiment showing all the relevant angles is found in Fig. 2. Here, $\gamma \sim 15°$ is the angle between acoustic tracks 1 and 2; $\alpha_{1,2}$ are the angles between tracks 1 or 2 and the wave front of the IS correspondingly; these angles can be found if we know angle α, so that $\alpha_1 \sim 78°$ and $\alpha_2 \sim 63°$.

The velocities of the IS along acoustic tracks 1 and 2 can be calculated using the $v_{1,2} = v/\sin\alpha_{1,2}$. The corresponding predominating frequencies of fluctuation for the two acoustic tracks are then $\Omega_c^{1,2} = v/(D_c \sin\alpha_{1,2})$, For the sound speed profile in the SW06 area, $D_c \sim 2hc_1/\sqrt{c_2^2-c_1^2} + 2\Delta h\sqrt{c_2^2-c_1^2}/\Delta c$. For parameters in SW06 area $D_c \sim 640$ m. Calculations give for frequencies $\Omega_c^1 \approx 3.45$ cph and $\Omega_c^2 \approx 3.8$ cph. These values are very close to the measured ones. We remark that these values are sensitive to the value of the ray cycle distance. However, the ray cycle can be effectively excluded by considering only the ratio of the predominating frequencies

$$\Omega_c^1/\Omega_c^2 = \sin\alpha_2/\sin\alpha_1. \tag{5}$$

For our case, this ratio is $\sin\alpha_2/\sin\alpha_1 \sim 0.91$ and for the experimental data it is $\Omega_c^1/\Omega_c^2 = 0.895$, close to the aforementioned ratio.

4. Summary

In summary, we see that the IS, moving approximately along an acoustic track, interacts with the quasiperiodical spatial interference pattern of the sound field formed by a set of rays (in the

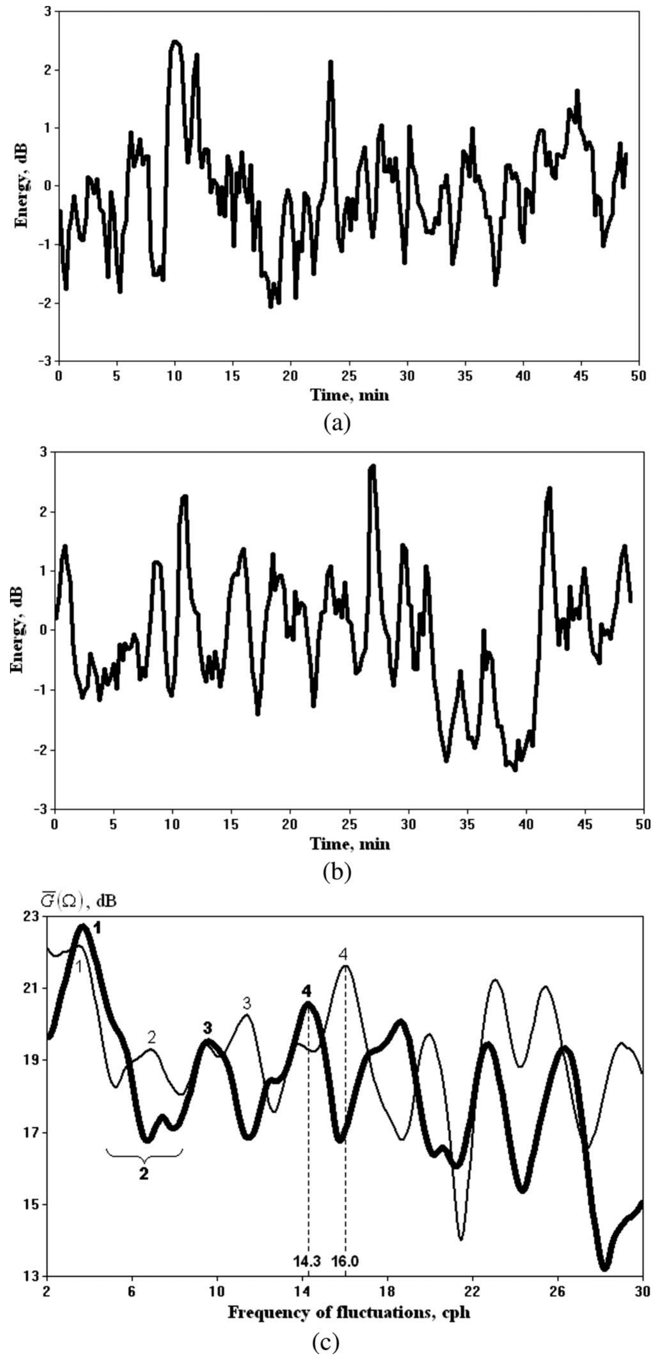

Fig. 4. Temporal dependence of the energy of the sound pulses for SHRU1 (a) and SHRU2 (b) for the time period 13 August 2006, 15:31–16:20 GMT. (c) Spectra of fluctuations of pulse energy. Bold line denotes spectrum for SHRU1, thin line corresponds to SHRU2. Dotted lines denote positions of the fourth harmonics of predominating frequencies.

high frequency approximation) radiated from the source in a shallow water waveguide. Correspondingly, the frequency of the temporal fluctuations of the sound intensity at the receiver is proportional to the velocity of the IS along the acoustic track. The difference in spectra of these fluctuations (the shift of the predominating frequencies) for two acoustic tracks depends on the angle between them and the observations reported here are consistent with this hypothesis.

It is very interesting that the value of the predominating frequency does not depend (or depends weakly) upon the shape and amplitude of the IS, and on how many separate peaks there are in the train, and on its exact position between source and receiver. It is just this circumstance that allows us to get comparatively good agreement between theory and experiment.

We note also that this effect can also be used for solution of the inverse problem—to diagnose parameters of moving solitons (velocity and direction) on the basis of acoustical measurements with high (mid) frequency sources and two differently directed acoustic tracks.

Acknowledgments

The authors are very grateful to D. J. Tang for the information about the radiated signals and helpful discussions. This work was supported by the Office of Naval Research (ONR), the Russian Foundation for Basic Research (RFBR), Grant No. 06-05-64853, and CRDF (REC 010).

References and links

[1]M. Badiey, Y. Mu, J. Lynch, J. R. Apel, and S. Wolf, "Temporal and azimuthal dependence of sound propagation in shallow water with internal waves," IEEE J. Ocean. Eng. **27**, 117–129 (2002).

[2]V. Grigorev and B. Katsnelson, "Fluctuations of high frequency acoustic signals in shallow water due to motion of internal soliton," Acoust. Phys. **54**, N6 (2008).